The physicochemical properties of Portland cement blended with calcium carbonate with different morphologies as a supplementary cementitious material

Lewis J. McDonald[1], M. Ara Carballo-Meilan[1],
Ricardo Chacartegui[2] Waheed Afzal[1]*
l.mcdonald.18@abdn.ac.uk, maria-ara.carballo-meilan@abdn.ac.uk,
ricardoch@us.es, waheed@abdn.ac.uk*
[1] School of Engineering, University of Aberdeen, Aberdeen,
United Kingdom, AB24 3UE
[2] Energy Engineering Department, University of Seville, Seville,
Spain, 41004
* Corresponding author

Abstract

This study proposes the addition of calcium carbonate produced using mineral carbon capture and utilisation technologies to reduce carbon emissions of Portland cement manufacturing from 0.96 $kgCO_2/kg$ of Portland cement to 0.33 $kgCO_2/kg$ of Portland cement with comparable strengths. This study reviews

the impact of calcium carbonate addition on properties of cement based on the available literature. Experimental findings are presented on how the addition of different polymorphs of calcium carbonate influence physicochemical behaviour of Portland cement in terms of hydration chemistry, compressive and flexural strength and thermal analysis. Three polymorphs of calcium carbonate (amorphous, micro calcite and nano calcite) are studied. This study reports the impact of three different calcium cabronate polymorphs especially that in the amorphous form. The addition of $CaCO_3$ in Portland cement can increase the compressive strength by about 20%. Examining the hydration shows the possibility formation of scawtite and tilleyite with competing effect on the product strength during hydration. Formation of 8 mass% of combined scawtite-tilleyite phases at ambient conditions using $CaCO_3$ is a new discovery; it results first in an increase in compressive strength and then, above 8 mass% it negatively impacts compressive strength. This study also provides avenues to use calcite as a sustainable supplementary cementitious material to reduce carbon emissions as well as improve early strengths.

Graphical Abstract

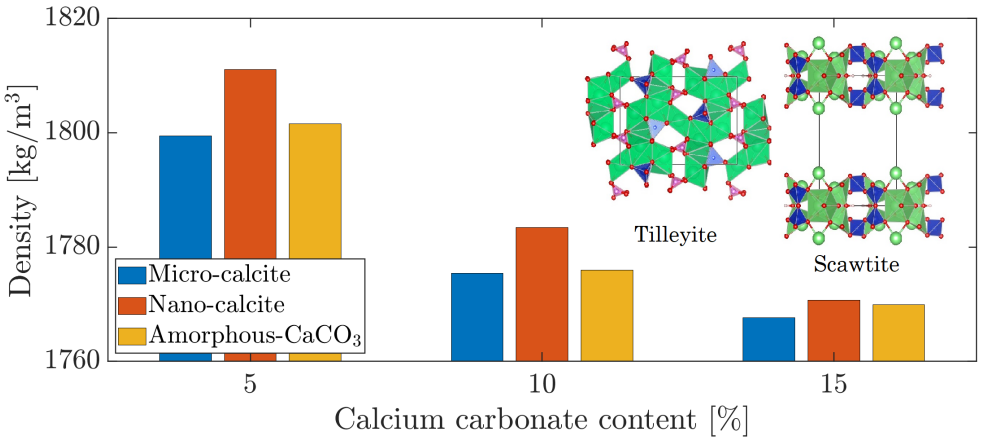

Keywords

Carbon Capture and Mineralisation; Calcium Carbonate; Portland Cement; Life-cycle Assessment; Cement Hydration

Highlights

- Mineralisation if CO_2 can produce calcium carbonates for Portland cement substitution
- CO_2 from Portland cement can be reduced from 0.96 kg_{eq}/kg cement to 0.33 kg_{eq}/kg cement
- Calcium carbonates change the hydration of Portland cement
- Compressive strength improves when micro- and nano-scale calcium carbonate are added
- Amorphous calcium carbonate reduces the compressive strength of Portland cement

Nomenclature

OPC	Ordinary Portland cement
PLC	Portland-limestone cement
SCM	Supplementary cementitious material
w/s	Ratio of water to solids (Portland cement & additives) of a cement paste
AFm	$Ca_2(Al,Fe)(OH)_6 \cdot X \cdot yH_2O$
Calcium Hemicarboaluminate	$3CaO \cdot Al_2O_3 \cdot 0.5CaCO_3 \cdot 11.5H_2O$
Calcium Monocarboaluminate	$3CaO \cdot Al_2O_3 \cdot CaCO_3 \cdot 11H_2O$
Tilleyite	$Ca_5(Si_2O_7)(CO_3)_2$
Scawtite	$Ca_7(Si_3O_9)_2CO_3 \cdot 2H_2O$
C	CaO
S	SiO_2
A	Al_2O_3
F	Fe_2O_3
H	H_2O
C-S-H	Calcium Silicate Hydrate
LCA	Life cycle assessment
XRD	X-ray diffraction
TGA	Thermogravimetric analysis
DSC	Differential scanning calorimetry

1 Introduction

Portland cement production is a major source of CO_2 emissions. The production of one tonne produces 950 kg of CO_2. Each year more than 4 billion tonnes of cement are produced worldwide (USGS, 2018), this accounts for 8% of all anthropogenic CO_2 (Lehne and Preston, 2018). In addition to the CO_2, other gases (NOx and SOx) and cement kiln dust (15-20% of the mass of clinker) are produced in the process of making Portland cement, all of which have a negative impact on the environment (Huntzinger and Eatmon, 2009). Reducing the clinker factor of Portland cement is currently used to offset the CO_2 emissions (Lothenbach et al., 2011), clinker is replaced with limestone and supplementary cementitious materials (SCM) prior to grinding which have a lower environmental impact than Portland cement (Miller, 2018). The reduced clinker factor is directly correlated with a reduced amount of clinker production. By careful selection of SCMs, the production process can be made more sustain-

able (Scrivener et al., 2018). The primary source of the CO_2 emissions is the cement kiln. Approximately 50% of the emission come from the calcination process (Eq. 1) and 40% from the burning of fuels to heat the kiln (Boesch and Hellweg, 2010). All other processes are responsible for the remaining 10%. This study presents a means to capture CO_2 from the calcination process through mineralisation and recycling it back into the cement production process as a SCM with the aim to create a sustainable Portland cement. The proposed capture method can be applied to both the kiln and the burning of fuels.

$$CaCO_3(S) \xrightarrow{heat} CaO(s) + CO_2(g) \tag{1}$$

Limestone has been used as an admixture for Portland cements for several decades to reduce the environmental impact as it is readily available, inexpensive and has low associated emissions (Imbabi et al., 2012). EN 197-1 (EN 197-1:2011, 2011) permits Portland-limestone cements (PLC) to contain up to 35% limestone, composed of a minimum 70% $CaCO_3$. At the higher end of the replacement limit, there is a reduction in mechanical properties making it unsuitable in some construction applications but has a lower water demand and is used to produce self-levelling concretes (Detwiler and Tennis, 1996). While adding calcium carbonate to Portland cement is not new, the effects of calcium carbonate, especially amorphous-$CaCO_3$ are not studied in enough detail to determine if its role is as a filler or as a reactant. Portland cements blended with upto 35% limestone or SCMs have overtaken OPC in terms of market share (Schmidt et al., 2013). The grinding of limestone is the primary source of carbon emissions associated with its use: 24-90 kg CO_2/tonne depending on final particle size (Kim et al., 2018) while the other miscellaneous processes are approximated to emit 2.76 kgCO_2/tonne by Kittipongvises (2017) as well as lower emissions of other pollutants such as NOx and SOx as detailed in their compre-

hensive analysis of limestone quarrying operations (Kittipongvises, 2017). By producing calcium carbonate directly from the Portland cement emissions it is believed that greater reductions of CO_2 emissions compared to limestone can be achieved.

The calcium carbonate in the limestone is known to react with tricalcium aluminate (C_3A) to form carbonate-AFm (Voglis et al., 2005) which forms denser a denser cement matrix, the reaction is limited by the C_3A content of the Portland cement and calcium carbonate added in excess is inert (Matschei et al., 2007). Further reaction of calcium carbonate with cement pastes may be possible with Péra et al. (1999) observing an unidentified calcium carbosilicate phase after hydration.

This study aims to assess the mechanical properties, rheological effects and hydration of calcium carbonate blended cements, with focus on the morphology and grain size of the calcium carbonate. The calcium carbonates differ from traditional limestone in that their particles are not subject to stresses from grinding and their altered size and morphology leads to potential for a new regime of reactivity. Calcium carbonate can be mineralised from CO_2 emissions and used as a mineral addition to Portland cement. The use of amorphous-$CaCO_3$ as a cement additive is novel to this study. It is produced through a simple precipitation reaction that was adapted from a previous study by McDonald et al. (2019) and McDonald et al. (2022).

The mineralisation process can be used to control the grain size and morphology of the calcium carbonate. The CO_2 sequestered in the mineralised calcium carbonate can potentially reduce the emissions from 0.96 $kgCO_{2eq}/kg$ to as little as 0.3 $kgCO_{2eq}/kg$, depending on the carbon capture method utilised (Batuecas et al., 2021). Through controlling the ageing time of the calcium carbonate and pH of the calcium source in the precipitation process, amorphous calcium

carbonate can be produced which has not been added to Portland cement as an additive. The potential benefits of amorphous calcium carbonate are that it readily crystallises when exposed to heat such as during hydration of Portland cement.

The use of a calcium carbonate produced from CO_2 emissions would require a carbon output to be less than that of limestone in order to be a suitable replacement. At first glance, calcium carbonate produced from CO_2 appears to be carbon-negative, however, each capture process has its own associated emissions that are obfuscated by the processes operating CO_2 input. A life cycle assessment has been conducted for the carbon capture process to evaluate the CO_2 reduction potential of freshly calcium carbonate.

2 Materials and Methods

2.1 Portland Cement

A commercial ordinary Portland cement (OPC) supplied by Hanson Cement was used. The manufacturer arranged to grind clinker with normal gypsum but not to add limestone. The cement is therefore free of added calcium carbonate. The batch composition and the calculated mineralogy of the cements were determined by x-ray fluorescence (XRF) and Bogue calculation. The phase composition and mineralogy are shown in tables 1 and 2. A Portland-limestone cement was also used for comparison purposes. The chemical composition and mineralogy are shown in Tables 3 and 4.

2.2 Calcium Carbonate

Three calcium carbonates - micro-calcite, nano-calcite and amorphous-$CaCO_3$ - were prepared by precipitation reactions. Micro-calcite was produced from CO_2

and calcium-rich brine in a prototype carbon capture process at the University of Aberdeen. The carbon capture process used a gas mixture similar to that of cement kiln flue gas. The process used serves as the basis of the life-cycle assessment presented later in this study. Nano-calcite and amorphous-$CaCO_3$ were precipitated from the mixing of $CaCl_2$ and Na_2CO_3 molar solutions. For the amorphous-$CaCO_3$ precipitation, 0.1 mol/l NaOH was added to the $CaCl_2$ brine to increase the pH and retard crystallisation. The grain size of the calcites are directly related to the the ageing time of the calcium carbonate in the solution. Micro-calcite was aged for two hours and nano-calcite was aged for ten minutes. After ageing, the calcites were removed the supernate by filtering with a vacuum pump before being placed in an oven at 30°C for 12 hours. The amorphous-$CaCO_3$ required a modified $CaCl_2$ brine with an increased pH, achieved by adding a small quantity of NaOH such that the pH of the final solution was between 9.2 and 9.4. The amorphous-$CaCO_3$ was aged for four minutes before being filtered through the vacuum pump and was then placed in an oven at 30°C for three hours to dry the calcium carbonate without causing crystallisation.

The calcites are distinguished from each other by their particle sizes, micro-calcite with grain size between 1 and 11 μm and nano-calcite with grain size from 0.09 to 1.2 μm (Table 5). The amorphous $CaCO_3$ was the finest $CaCO_3$ used, with particles between 0.065 and 0.720 μm and was characterised by its lack of crystallinity defined from the appearance of the x-ray diffraction pattern using filtered copper Kα radiation. Figure 1 compares diffractograms obtained from micro- and nano-calcite with the amorphous-$CaCO_3$.

2.3 Blended Cements

OPC and freshly-precipitated $CaCO_3$ were blended using an electric mixer to produce nine cement blends, 5wt.%, 10wt.% and 15wt.% micro-calcite blend, 5wt.%, 10wt.% and 15wt.% nano-calcite blend and 5wt.%, 10wt.% and 15wt.% amorphous $CaCO_3$ blend. After blending the fineness of the cement powders was measured using the Blaine Air Permeability method (EN 196-6:2018, 2019). For rheological measurements blends were also made at 20% mass substitution, this was not done for compressive and flexural strength measurements due to the difficulty of the pastes to work with at this substitution level.

Standards consistency - the minimum water content at which all Portland cement particles are hydrated - was determined using a drop test with a 10 mm diameter plunger. Water was added to the pastes to produce a water/solids ratios (w/s) between 0.2 and 0.3 with a tolerance of 0.005. Mixing of the pastes was carried out in accordance with (EN 196-3:2005, 2005). Pastes were placed into conical moulds with bottom diameter of 80 mm, top diameter of 70 mm and a height of 40 mm. The base of the mould was a glass baseplate the plunger was dropped into the pastes until the w/s at which the distance between the dropped plunger and baseplate was between 4 and 8 mm.

Initial and final setting time of the cement pastes was measured using a Vicamatic 2 Automatic Setting Time Tester manufactured by Controls Group. The setting time measurements were conducted using pastes at their standard consistency. The same mixing time and moulds were used as in the consistency test. For initial setting time a 1.13 mm diameter needle was used and dropped into the cement pastes until the penetration depth was less than or equal to 37.5 mm. For final setting time, a needle with a 5 mm diameter attachment positioned 0.5 mm from the end of the needle was used. The final setting time was the point at which the needle penetrated the paste but the attachment left

no mark on the paste surface. As the apparatus recorded penetration depths nearing the initial and final setting limits, the time between measurements was reduced from every 5 minutes to every minute for initial set and from every 20 minutes to every 5 minutes.

For strength testing, the blends were hydrated with tap water to a w/s of 0.5. The w/s was chosen as 10% and 15% nano-calcite blends and all amorphous $CaCO_3$ blends produced unworkable mixes with reducing water content. The pastes were mixed using a MasterMix electric mixer until thoroughly combined.

2.4 Compressive Strength

Hydrated cement pastes were poured into 50x50x50 mm lightly-oiled steel moulds and subject to vibration to reduce air pockets. Each mould allowed for three cubes to be produced at a time. The pastes were left overnight at room temperature to harden before being removed from the moulds and placed into water baths and removed after 1, 3, 7 & 28 days from the time of casting. In total three cubes of each blend as well as OPC and each curing time were produced for a total of 111 cubes. Prior to compressive testing, cubes were removed from the water bath, surface dried and the cubes were weighed and the dimensions measured using callipers so that the bulk density could be calculated.

Compressive strength measurements were made using a uniaxial load method. Cubes were subject to an increasing load of 2000 N/s until failure. The compressive strength was calculated using equation 2:

$$\sigma_c = \frac{F_c}{bd} \tag{2}$$

where F_c is the compressive force at failure and b is the measured cube breadth and d is the measured cube width.

2.5 Flexural Strength

The process for preparing cement paste bars for flexural strength was the same as for compressive strength only the dimensions of the moulds used was 160x40x40 mm. In total 111 bars were produced for flexural tests.

Flexural tests were conducted using a three-point test method. The span between the lower rollers was 100 mm and the load was applied to the top surface midway between the lower rollers with a rate was 50 N/s until the bars failed and split in two. The flexural stress at failure was then calculated using equation 3:

$$\sigma_f = \frac{3}{2}\frac{F_f L}{d^3} \tag{3}$$

where F_f is the load at failure, L is the distance between spans and d is the bar cross sectional dimensions.

2.6 Cement Hydration

2.6.1 Sample Preparation

Cement blends were produced by combining calcium carbonates with ordinary Portland cement in a ratio of 1:9 by weight. Three blended cement mixes were produced, one for each calcium carbonate precipitated.

To produce samples, 20 grams of cement were hydrated with 10 grams of water and mixed by hand. The resulting paste were transferred to cubic moulds and an oiled glass plate was placed on the open surface to create an air tight seal and minimise carbonation from the atmosphere. The cubes were demoulded after 24 hours and placed into a water bath to cure. Samples were removed from the water bath after 7 and 28 days, ground by hand with a pestle and mortar to a fine powder for analysis.

2.6.2 X-ray Diffraction Method

X-ray diffraction was carried out using a Malvern Panalytical XPert Powder Diffractometer. The samples were placed into sample holders prepared such that a smooth powder surface was produced. The samples were then placed into the diffractometer where they were subject x-rays. The x-rays were produced from a copper radiation source with Kα wavelength of 1.54 Å. The angle between radiation source and detector continually increased with time from 5°2Θ to 60°2Θ. Analysis of the resulting patterns was conducted using the HighScore Plus which allowed for phase identification and Rietveld refinement of the XRD diffractograms.

2.6.3 Thermogravimetirc Analysis Method

Thermal analysis was conducted using a Mettler Toledo TGA/DSC 3+. 20-40 μg of samples were placed into alumina crucibles for analysis which was then lowered into the sample cell in the TGA/DSC furnace. The Mettler Toledo TGA/DSC 3+ allowed for the mass to be measured with temperature and time as well as the heat flow which allows for transition temperatures of phases to be detected. The heat flow is measured from the measured temperature difference between the sample cell and a reference cell throughout the analysis.

The method used to determine the thermal decomposition of the calcium carbonates and cement blends was developed to cover three main decomposition ranges (Bhatty, 1986): 100-400°C, dehydration evaporation of water and release of structural water; 400-600°C, dehydroxilation, the decomposition of $Ca(OH)_2$; 600-800°C, decarbonation, the liberation of CO_2 (Dweck et al., 2000). The samples were subjected to a heating rate of 20°C per minute from 25°C to 900°C as suggested by Pane and Hansen (2005). The decomposition of calcium silicate hydrate (C-S-H) takes place continuously throughout this temperature

range (Shaw et al., 2000).The samples were then held at 900°C for ten minutes to monitor that the mass is stable. The heating was done in a nitrogen atmosphere at a flow rate of 50 ml/min to prevent reaction between the samples and air.

2.7 Life Cycle Assessment

A life cycle assessment of calcium carbonate blended cements produced from cement kiln emissions has been conducted.

2.7.1 Scope

The process of producing Portland cement blended with calcium carbonate is broken down to four primary stages:

1. Raw materials acquisition – This includes the quarrying and initial processing of raw materials such as transport, grinding, blending and granulation

2. Kiln process - This process covers the activity taking place within the kiln from input of prepared materials to cooling of clinker

3. Carbon capture process – This covers the process where CO_2 captured and remineralised to calcium carbonate

4. Post-kiln treatment – These treatments are the grinding of clinker nodules and introduction of additives to the Portland cement including calcium carbonate

These stages are shown in detail in figure 2.

The current CO_2 capture method uses sodium hydroxide solution during the capture stage. The sodium hydroxide reacts with the CO_2 to form Na_2CO_3. As the capture process is not perfectly efficient, a portion of flue gases are

discharged to the atmosphere. The Na_2CO_3 solution is then combined with calcium rich brine, $CaCl_2$ is the calcium source used in the lab, which leads to the precipitation of $CaCO_3$. The sodium hydroxide is the most carbon intensive material in the capture process. Two sodium hydroxide production methods are considered in this life-cycle assessment: Scenario 1 - diaphragm cell electrolysis method and scenario 2 - membrane cell electrolysis method (Crook and Mousavi, 2016). An alternative to sodium hydroxide is also considered, scenario 3 - ammonia is used instead which is then regenerated after $CaCO_3$ precipitation through heating of the resulting ammonium chloride to form ammonia gas and hydrochloric acid. The ammonia is separated from the hydrogen chloride and is then reused. The regeneration has higher energy requirements but a lower molar volume of ammonia is required compared to sodium hydroxide.

2.7.2 Life Cycle Inventory

Ordinary Portland Cement Production The functional unit for the OPC production is 1 kg of OPC. Conveniently the emissions of CO_2 to air (approx. 0.45 kg/kg Portland cement) from the cement kiln is close to the required CO_2 to produce 1 kg of $CaCO_3$ (0.44 kg). The dataset used for Portland cement is *Portland cement (CEM I), CEMBUREAU technology mix, CEMBUREAU production mix, at plant, EN 197-1 RER S*. The data set obtained from the Ecoinvent database 3.1 and is representative of several plants producing CEM I Portland cement. The data has been reviewed, validated by CEMBUREAU and carried out in accordance with ISO 14040.

Capture Process The functional unit for the capture processes is 1 kg of calcium carbonate produced. The inputs required required are shown in Table 6. The quantities of electricity required for scenarios 1 and 2 are calculated based on an estimated sequestration of 200 kg per day of CO_2 by the prototype carbon

capture unit used to produce calcium carbonates. The electricity required for scenario 3 is based on a theoretical modification to the prototype capture unit such that ammonia can be used to capture the CO_2 and is then regenerated after calcium carbonate precipitation.

3 Results and Discussion

3.1 Blaine Fineness

The surface area of ground Portland cement with calcium carbonate substitutions increases (Table 7), which is to be expected as the particles size of all calcium carbonates used is smaller than that of the OPC. The greatest increase in surface area is seen when 15% of the cement is substituted with amorphous-$CaCO_3$. The surface area is directly related to the calcium carbonate grain size. With decreasing grain size and increasing calcium carbonate content the surface area increases.

3.2 Standard Consistency and Setting Times

The standard consistencies, initial and final setting times are presented in Table 8. Inclusion of all forms of calcium carbonate used increases the required water to fully hydrate the cement compared to both OPC and PLC. The water requirement increases as the particle size of the calcium carbonate decreases.

Both the initial and final setting times of the calcium carbonate blends decreases compared to OPC with smaller calcium carbonate particles and increasing calcium carbonate content causing a greater decrease in setting time. The PLC used had the greatest setting time. The setting times of the calcium carbonates are lower than the allowed 45 minutes of EN197-1. This is a potential limitation of the blends, although it can be overcome using setting-time

retarders. This is potentially due to the increased water requirement to reach the standard consistency being available for hydration and the substitution of calcium carbonate which does not react with water. This is in contrast to limestone additives which reduce the water requirement due to their increased particle size and smaller surface area compared to ground Portland cement clinker (Tennis et al., 2011). The increased water demand, both during hydration and during precipitation of $CaCO_3$s has a negative impact on the sustainability of the $CaCO_3$ blends.

3.3 Compressive Strength Development

Compressive strength improved with the inclusion of micro- and nano-calcite (Figures 3 and 4). The compressive strength increase after 28 days in both calcite-blends follows a parabolic increase in strength with increasing calcite content. The optimum content to improve compressive strength for both calcite-blends was 10%. 10% nano-calcite cured for 28 days had the greatest strength increase compared to OPC it was 27% higher (Figure 5). Strength gain is thought to be from two sources: firstly, the smaller particle sizes of the calcites provide a filler effect and reduce the pore spaces. Secondly, the calcite particles act as nucleation points for the formation of both CH and C-S-H and improve the binding of the cement matrix (Mohamed et al., 2015). Poudyal and Adhikari (2021) also observed an increase in compressive when incorporating nano-calcite to Portland cement. The authors attribute the improved strength to a denser pore structure as well as increased hydration products which is in-line with the findings presented in this study.

Amorphous-$CaCO_3$ showed an increase in compressive strength after 28 days at 5% inclusion (Figure 6), at higher substitution the strength decreased linearly (Figure 5). The decrease in strength of amorphous-$CaCO_3$ blended cement is

thought to be from agglomeration of amorphous-$CaCO_3$ particles (Figure 8). Additionally residual water in the amorphous-$CaCO_3$ due to the reduced drying period compared to the calcite may have played a role and effectively increased the w/s. Further drying of amorphous-$CaCO_3$ led to a mass loss of 8% and complete crystallisation of the sample.

The compressive strength of the benchmark Portland-limestone cement containing 18.27% ground calcium carbonate was tested and is presented in Figure 7. The calcium carbonate cements outperform the commercially available PLC in compressive strength. Improved compressive strength allows for structural members of reduced sectional dimensions to be produced leading to further reduction in Portland cement required to achieve the same member strength. The reduced cement production will have a net positive impact on the emissions associated with the production of $CaCO_3$ Portland cement blends.

3.4 Flexural Strength Development

$CaCO_3$ had very little effect on flexural strength. Each blend performed slightly better than OPC for all substitution levels and curing time as shown in figures 9, 10 and 11, however, the increase in flexural strength is minimal and falls within the 5% margin of error. As the flexural strength is not changed, the use of steel reinforcement is still necessary for load-bearing members to prevent failure in tension and no reduction to the size of reinforcement compared to OPC could be achieved.

3.5 Bulk Density

Hydrated bulk densities for each blend after 28 days are presented in figure 12. For all blends the bulk density was greater than that of OPC, which was 1760 kg/m^3. With increasing $CaCO_3$ content, the bulk density of the blends

decreased. Nano-calcite produced the densest blends for all substitution levels, followed by micro-calcite.

3.6 Cement Hydration

3.6.1 X-ray Diffraction Results

XRD analysis of the cement samples showed that hemi- and monocarboaluminate form during hydration when calcium carbonate is present. This occurs in both the PLC and the calcium carbonate blended cements. Hemicarboaluminate forms within the first 7 days of hydration (figure 13), whereas monocarboaluminate forms within 28 days from crystallisation of hemicarboaluminate (figure 14).

Consistent to our earlier work, (McDonald et al., 2022), two silicocarbonates formed when nano-calcite was present. These phases were identified as tilleyite and scawtite. Both were present after 7 and 28 days. These phases are uncommon, typically only found in extreme temperature and pressure conditions such as in oil well cements (Eilers et al., 1983) or when highly-soluble carbonates are added to Portland cement as demonstrated by Medvešček et al. (2006). The formation of these silicocarbonates is indicative of an increased reactivity of calcium carbonates compared to limestone additions. The formation of these phases may be what contributes to the increased strength of the nano-calcite blend as they have a higher density than that of other cement hydrates. The crystal structure of tilleyite (figure 15) closely resembles that of C-S-H (Gard and Taylor, 1976; Richardson, 2004). It is believed that the carbonate from nano-calcite is available in solution to react with C-S-H during hydration leading to tilleyite formation which then converts to scawtite with continued hydration. For comparison the crystal structure of scawtite is shown in figure 16.

3.6.2 Thermogravimetric Analysis Results

Thermals analysis of the calcium carbonates is shown in figure 17. The calcites showed no sign of structural water, as expected (figures 17(a) and (b)). However the amorphous $CaCO_3$ (figure 17(c)) was found to have a water content of 13% by mass. Each calcium carbonate lost approximately 44% of their mass between 700 and 800°C which is the CO_2 being liberated and corresponds to a negative change in the heat flow, it is exothermic. Additionally there is a small exothermic peak at 690°C in the heat flow of the amorphous-$CaCO_3$ indicating that a phase change is occurring, likely the transition from amorphous to crystalline calcium carbonate.

After 7 days of hydration OPC shows three periods of decomposition corresponding to dehydration, dehydroxilation and decarbonation (figure 18(a)). The dehydration is the largest mass loss at 11%. Little decarbonation occurs due to the lack of added carbonate what does occur is due to atmospheric absorption of CO_2 during the curing process. Similarly, PLC has three periods of decomposition with a considerably larger decarbonation period (figure 18(b)). The dehydration is once again the largest mass loss at 12%, followed by the decarbonation at 6%. The heat flow of both the OPC and PLC indicates that the three decomposition periods are exothermic. The dehydroxilation of the OPC and PLC is are similar indicating that the presence of ground calcium carbonate does not contribute greatly to calcium hydroxide formation.

After 28 days of hydration the OPC has hydrated considerably larger mass loss due to dehydration of 23% (figure 19(a)). The increased water content is due to the further reaction of clinker during the longer hydration period. The decarbonation is again very little. The PLC has also hydrated further indicated by a mass loss of 16% during the dehydration period (figure 19(b)). The lower mass loss compared to OPC is a consequence of the calcium carbonate content

of 18% being unreactive with water. Dehydroxilation of OPC and PLC are once again similar.

After 7 days of hydration the mass loss of all three calcium carbonate blends is similar as shown in figure 20. However, the heat flow differs between the calcium carbonate blends. Micro-calcite has the highest between 200 and 600°C (figure 20(a)) followed by the amorphous-$CaCO_3$ blend (figure 20(c)) and lastly the nano-calcite blend (figure 20(b)). For each calcium carbonate blend, the dehydroxilation accounts for 3% of the total mass loss, indicating that the calcium carbonates do not behave differently in regards to calcium hydroxide formation. This is similar to the OPC and PLC which have dehydroxilation of 2% and 3% respectively. All calcium carbonate cements show similarities in both mass loss and heat flow to PLC after 7 days of hydration.

The micro-calcite blend has the greatest mass loss due to dehydration mass loss after 28 days of 22% as well the greatest overall mass loss of 38% (figure 21(a)), the nano-calcite blend has the second highest dehydration mass loss of 13% (figure 21(b)) and the amorphous-$CaCO_3$ blend had the lowest mass loss of only 9% (figure 21(c)). Both the nano-calcite and amorphous-$CaCO_3$ blend had an overall mass loss of 31%. Consequently, the heat flow during dehydration follows the same trend. The differences in dehydration indicate that the smaller sized calcium carbonates are having an effect on the hydration of the cement pastes. This is speculated to be due to pore filling effects of the particles which prevent water penetrating into the pastes. Again the dehydroxilation is similar to those of OPC and PLC at the same hydration period. The decarbonation of the calcium carbonate blends follows the same trend as the dehydration where the micro-calcite blend has the highest, followed by the nano-calcite blend and lastly the amorphous-$CaCO_3$ blend.

3.7 Life Cycle Assessment

The impact assessment examines the production methods of OPC and calcium carbonate in fourteen categories described in Table 9 using the ICLD 2011 midpoint+ method available in SimaPro.

3.7.1 Ordinary Portland Cement Production

The associated environmental impact of the production of 1 kg of Portland cement is show in table 10. The production of Portland cement is a considerable pollutant with a climate change impact of 0.899 kg CO_2eq/kg. This value includes the substitution of upto 5% of the cement clinker with minor additives such as gypsum and limestone which have a lower kg CO_2eq/kg than cement clinker. The value for climate change impact is comparable to those determined by Lehne and Preston (2018) and Batuecas et al. (2021) who estimate that the CO_2 potential of Portland cement is 0.93 and 0.96 kgCO_2/kg cement, respectively.

3.7.2 Capture Process

The production method of the sodium hydroxide is the main source of CO_2 during the capture process for scenarios 1 and 2. Using the more common diaphragm cell electrolysis method (Table 11) leads to global warming potential of 0.667 kgCO_2 equivalent. For comparison, the membrane cell electrolysis method (Table 12) has a lower global warming potential of 0.154 kgCO_2 equivalent.

Scenario 3 (Table 13) has a global warming potential of 0.244 kgCO_2 equivalent. This is better than that of scenario 1 however the higher energy requirements for ammonia regeneration contributes more to climate change, human toxicity (non-cancer effects & cancer effects), particulate matter, land usage, freshwater toxicity and water resource depletion than scenario 2. However, sce-

nario 3 has a lower impact in the other 7 out of 14 categories assessed.

3.7.3 Calcium carbonate blended Portland cement

During the grinding process, the dried calcium carbonate is incorporated into the Portland cement. A study into the change in compressive strength and rheology of the calcium carbonate blended Portland cement has shown that upto upto 15% of the mass of the Portland cement clinker can be substituted with moderate improvement in strength as shown in Section 3.3. At 10% substitution the maximum compressive strength increase is observed, a change of 27% compared to the OPC. As the amount of calcium carbonate is more than the amount that is able to be used as an additive without hindering the mechanical properties, an excess of calcium carbonate will be obtained which can then be used in other product streams such as paper manufacturing and agriculture.

3.7.4 Results and Interpretation

Of the 0.902 kg of CO_2 equivalent produced during the manufacture of Portland cement 0.885 kg of CO_2 are emitted directly to the atmosphere. Approximately 50% of the atmospheric emissions are released from the cement kiln (Lehne and Preston, 2018) which is conveniently close to the 0.44 kg of CO_2 required to produce 1 kg of calcium carbonate. As such there is an excess of calcium carbonate produced per kg of Portland cement, which if utilised in other industries where calcium carbonate is valuable such as the manufacture of paint, paper and plastics.

Assuming that the calcium carbonate is entirely used in some manner, a Portland cement blend with a 15% clinker substitution is therefore responsible for 0.327 kgCO_2eq/kg, a 64% reduction, when the sodium hydroxide for the capture process is produced using the membrane cell hydrolysis method (Scenario 2, Table 12). This reduction is comparable to that of Batuecas et al.

(2021) who found a reduction to 0.3 $kgCO_2$/tonne of Portland cement using a ionic liquid based carbon capture method. While it is possible to add more calcium carbonate according to the European Standard (EN 197-1:2011, 2011), 15% was used in this calculation as it provides near equivalent strength to that of the OPC considered in this study. Comparatively the associated emissions of ground limestone range from 24.5-90.7 $kgCO_2$/kg of limestone, depending on grind quality (Kim et al., 2018). At 15% limestone substitution this would equate 0.77-0.78 $kgCO_2$/kg of blended cement dependent on grind quality. The near equivalent strength allows for 15% calcium carbonate blends to be used in all situations where OPC is typically used. Poudyal and Adhikari (2021) suggests that the lifespan of structures built with $CaCO_3$ Portland cements is extended leading to further environmental impact reduction from construction and maintenance.

While the climate change potential of Portland cement is reduced by blending with calcium carbonate, many of the other categories are increased. The most notable increases are the ozone depletion, human toxicity (non-cancer and cancer effects), freshwater eutrophication, freshwater ecotoxicity and mineral, fossil & renewable resource depletion, where the difference is orders of magnitude greater than that of Portland cement.

To achieve optimum reduction in CO_2, the medium used to capture the CO_2 is the most important factor. While this assessment focused on the usage of NaOH as it was readily available for the prototype capture unit, the production method of the NaOH has considerable impact. The modern process, using membrane cell electrolysis, (scenario 2) provided the best outcome.

Usage of ammonia where it can be regenerated and reused (scenario 3) as the capture medium also provides significant CO_2 reduction. The reduction is not as favourable as that of scenario 2 due to higher electricity requirements. The

electricity consumed is based on UK average electricity generation. Approximately 40% of UK electricity generation is from highly CO_2 intensive fossil fuel (DUKES, 2020). Due to a decreasing trend in fossil fuel usage in favour of renewables, this scenario may become more viable than scenario 2 in the future.

4 Practical Implications of the Present Study

The use of sodium hydroxide as the capture medium is the main limiting factor of this study. Sodium hydroxide was used as the capture medium in this study due to its availability. There is improvement potential in the capture method used, such as using a regenerative capture medium. Ammonia was considered in this study as it can be regenerated and reused with the application of heat. Doing so required more electricity which ultimately lead to a higher CO_2 output than that of NaOH produced using the membrane cell method.

A second practical implication of this study is the implementation of the carbon capture technology to cement kilns. The present study used a prototype capture device that used a gas mixture resembling cement kiln flue gas. The capture capacity of the device was upto 200 $kgCO_2$ per day where as modern cement plants are capable of producing thousands of tonnes of cement per day and consequently thousands of tonnes of CO_2. Scalability of the capture process has not been implemented at present.

5 Limitation of the Present Study

The principle limitation of the present study is the narrow scope of Portland cement life-cycle data. The data used is representative of a typical Ordinary Portland cement production process in the European Union. Using a larger number of data sets would allow for better comparison to global cement pro-

duction.

6 Conclusions and Prospects

The mineralisation of CO_2 to $CaCO_3$ for use as a Portland cement admixture has lead to altered properties of the cement pastes. The controlled morphology and grain size of the $CaCO_3$ have differing effects to $CaCO_3$ from ground limestone.

The surface area of Portland cement is increased by adding calcium carbonates. The increase in surface increases the water required to fully hydrate the calcium carbonates. This is due to the increased dispersion of the water around the finer particles. Calcium carbonate reduces both the initial and final setting time with a larger reduction observed as calcium carbonate size decreases.

Compressive strength is improved by the inclusion of micro- and nano-calcite for all substitution levels compared with OPC. 10% nano-calcite blend after 28 days had the highest compressive strength at 58.3 MPa, 27.3% higher than OPC. On the other hand amorphous-$CaCO_3$ increased the strength when 5% was added but at higher substitution the strength was lower than that of OPC. For comparison the compressive strength of a PLC containing 18.27% calcium carbonate. The PLC exhibited the lowest strength of all cement blends tested.

Flexural strength is unaffected by the inclusion of $CaCO_3$. This is due to the shape of the calcium carbonates imparting no mechanical benefit in tension. Bulk density of $CaCO_3$ blends increased compared to that of OPC, higher bulk density was achieved at lower substitution (5%) and decreased as more Portland cement was substituted.

The addition of calcium carbonates leads to the formation of carboaluminate phases through reaction with C_3A, the same reaction pathway that limestone reacts with Portland cement. Additionally, nano-calcite forms the silicocarbonates tilleyite and scawtite through dissolved carbonate reacting with C-S-H.

The formation of tilleyite and scawtite at ambient conditions in calcium carbonate Portland cements is believed to be novel and is representative of increased reactivity of calcium carbonates compared to ground calcium carbonate from limestone. Their formation is thought to lead to a denser cement matrix due to their higher density compared to the common Portland cement hydration phases. The increased density is what is believed to improve mechanical properties as the tilleyite and scawtite do not show cementitious properties.

The life cycle assessment has found that the amount of CO_2 from Portland cement production can be significantly lowered by implementing mineral carbon capture and utilisation technology to the cement kiln. The reduction in CO_2 is equivalent to 67% of those of the manufacture of Portland cement if the calcium carbonate produced is entirely utilised. To achieve optimum reduction in CO_2, the medium used to capture the CO_2 is the most important factor.

In conclusion, calcium carbonate blended Portland cements with their altered hydration, mechanical properties, rheology and the lower environmental impact are an ideal candidate for the sustainable production of Portland cement. The precipitation of calcium carbonate from Portland cement emissions leads to a circular economy where the CO_2 is reintroduced to the process. The presented research has potential to reduce CO_2 emissions from Portland cement production, produces calcium carbonate that is already permitted in cement blends and requires no changes to legislation to permit its usage.

Contributions

Methodologies, experimental work and manuscript preparation by LJM, microcalcite precipitation and amorphous $CaCO_3$ precipitation method developed by M.-Ara CM. WA is the internal supervisor of LJM for their PhD studies and contributed to the discussion. RC contributed to the discussion.

Acknowledgements

The authors wish to dedicate this work to the memory of late Dr Mohammed Imbabi who along with Prof Fred Glasser contrbuted to the early discussions regarding mineral carbon capture and utilisation. LJM also wishes to thank Prof Fred Glasser for his advice and help in understanding mineralogy and cement chemistry. We also thank Dr Wanawan Pragot for fruitful discussions. Electron Microscopy was performed in the ACEMAC Facility at the University of Aberdeen.

Funding

This research did not receive any specific grant from funding agencies in the public, commercial, or not-for-profit sectors.

References

Batuecas, E., Liendo, F., Tommasi, T., Bensaid, S., Deorsola, F., and Fino, D. (2021). Recycling CO_2 from flue gas for $CaCO_3$ nanoparticles production as cement filler: A Life Cycle Assessment. *Journal of CO2 Utilization*, 45:101446.

Bhatty, J. I. (1986). Hydration versus strength in a portland cement developed from domestic mineral wastes — a comparative study. *Thermochimica Acta*, 106:93–103.

Boesch, M. and Hellweg, S. (2010). Identifying the improvement potentials in cement production with life cycle assessment. *Environmental Science Technology*, 44:9143–9149.

Crook, J. and Mousavi, A. (2016). The chlor-alkali process: A review of history and pollution. *Environmental Forensics*, 17(3):211–217.

Čuček, L., Klemeš, J. J., and Kravanja, Z. (2015). Overview of environmental footprints. In *Assessing and Measuring Environmental Impact and Sustainability*, pages 131–193. Elsevier.

Detwiler, R. and Tennis, P. (1996). *The use of limestone in Portland cement: A state-of-the-art review*. Portland Cement Association.

DUKES (2020). Digest of United Kingdom Energy Statistics 2020. National statistic, Department for Business, Energy & Industrial Strategy, London, UK.

Dweck, J., Buchler, P. M., Coelho, A. C. V., and Cartledge, F. K. (2000). Hydration of a Portland cement blended with calcium carbonate. *Thermochimica Acta*, 346(1-2):105–113.

Eilers, L., Nelson, E., and Moran, L. (1983). High-temperature cement compositions - Pectolite, scawtite, truscottite, or xonotlite: Which do you want? *Journal of Petroleum Technology*, 35:1373–1377.

EN 196-3:2005 (2005). Methods for Testing Cement: Part 3. Determination of Setting Time and Soundness. Standard, British Standards Institute, London, UK.

EN 196-6:2018 (2019). Methods of testing cement. Determination of fineness . Standard, British Standards Institute, London, UK.

EN 197-1:2011 (2011). Cement. Composition, specifications and conformity criteria for common cements. Standard, British Standards Institute, London, UK.

Gard, J. and Taylor, H. (1976). Caclium silicate hydrate (II) ("C-S-H(II). *Cement and Concrete Research*, 6:667–678.

Huntzinger, D. and Eatmon, T. (2009). A life-cycle assessment of portland cement manufacturing: Comparing the traditional process with alternative technologies. *Journal of Cleaner Production*, 17:668–675.

Imbabi, M., Carrigan, C., and McKenna, S. (2012). Trends and developments in green cement and concrete technology. *International Journal of Sustainable Built Environment*, 1:194–216.

Kim, Y.-J., Leeuwen, R., Cho, B.-Y., Sriraman, V., and Torres, A. (2018). Evaluation of the efficiency of limestone powder in concrete and the effects on the environment. *Sustainability*, 10:550.

Kittipongvises, S. (2017). Assessment of environmental impacts of limestone quarrying operations in thailand. *Environmental and Climate Technologies*, 20:67–83.

Lehne, J. and Preston, F. (2018). *Making Concrete Change: Innovation in low-carbon cement and concrete*. Chatham House, London.

Lothenbach, B., Scrivener, K., and Hooton, R. (2011). Supplementary cementitious materials. *Cement and Concrete Research*, 41:1244–1256.

Matschei, T., Lothenbach, B., and Glasser, F. (2007). The role of calcium carbonate in cement hydration. *Cement and Concrete Research*, 37:1465–1471.

McDonald, L., Imbabi, M., and Glasser, F. (2019). A new, carbon-negative precipitated calcium carbonate admixture for low-carbon portland cements. *Materials*, 12:554.

McDonald, L. J., Afzal, W., and Glasser, F. P. (2022). Evidence of scawtite and tilleyite formation at ambient conditions in hydrated portland cement blended

with freshly-precipitated nano-size calcium carbonate to reduce greenhouse gas emissions. *Journal of Building Engineering*, 48:103906.

Medvešček, S., Gabrovšek, R., Kaučič, V., and Meden, A. (2006). Hydration products in water suspension of portland cement containing carbonates of various solubility. *Acta Chimica Slovenica*, 53:172–179.

Miller, S. (2018). Supplementary cementitious materials to mitigate greenhouse gas emissions from concrete: can there be too much of a good thing? *Journal of Cleaner Production*, 178:587–598.

Mohamed, A. R., Elsalamawy, M., and Ragab, M. (2015). Modeling the influence of limestone addition on cement hydration. *Alexandria Engineering Journal*, 54(1):1–5.

Pane, I. and Hansen, W. (2005). Investigation of blended cement hydration by isothermal calorimetry and thermal analysis. *Cement and Concrete Research*, 35(6):1155–1164.

Péra, J., Husson, S., and Guilhot, B. (1999). Influence of finely ground limestone on cement hydration. *Cement and Concrete Composites*, 21(2):99–105.

Poudyal, L. and Adhikari, K. (2021). Environmental sustainability in cement industry: An integrated approach for green and economical cement production. *Resources, Environment and Sustainability*, 4:100024.

Richardson, I. (2004). Tobermorite/jennite- and tobermorite/calcium hydroxide-based models for the structure of C-S-H: applicability to hardened pastes of tricalcium silicate, β-dicalcium silicate, Portland cement, and blends of Portland cement with blast-furnace slag, metakaolin, or silica fume. *Cement and Concrete Research*, 34(9):1733–1777.

Schmidt, W., Radlinska, A., Nmai, C., Buregyeya, A., Lai, W., and Shicong, K. (2013). Why does Africa need African concrete? An observation of concrete in Europe, America, and Asia – and conclusions for Africa. In *International Conference on Advances in Cement and Concrete Technology in Africa*.

Scrivener, K., John, V., and Gartner, E. (2018). Eco-efficient cements: Potential economically viable solutions for a low-CO_2 cement-based materials industry. *Cement and Concrete Research*, 114:2–26.

Shaw, S., Henderson, C., and Komanschek, B. (2000). Dehydration/recrystallization mechanisms, energetics, and kinetics of hydrated calcium silicate minerals: an in situ TGA/DSC and synchrotron radiation SAXS/WAXS study. *Chemical Geology*, 167(1-2):141–159.

Tennis, P., Thomas, M., and Weiss, W. (2011). State-of-the-art report on use of limestone in cements at levels of up to 15%. *PCA R&D SN3148, Portland Cement Association, Skokie, IL*.

USGS (2018). *USGS Minerals Yearbook*. U.S. Department of the Interior.

Voglis, N., Kakali, G., Chaniotakis, E., and Tsivilis, S. (2005). Portland-limestone cements. their properties and hydration compared to those of other composite cements. *Cement and Concrete Composites*, 27(2):191–196.

7 Tables and Figures

Table 1: Chemical composition determined using XRF of Portland cement used.

Chemical Composition	Phase Wt. %
SiO_2	20.28
Al_2O_3	4.71
Fe_2O_3	3.27
CaO	67.13
SO_3	2.54
MgO	0.67
K_2O	1.40

Table 2: Mineralogy of Portland cement used.

Mineralogical Composition	Phase Wt. %
C_3S	59.65
C_2S	15.24
C_3A	11.81
C_4AF	8.65
C\$$H_2$	4.65

Table 3: Chemical composition determined using XRF of Portland-limestone cement used. CO_2 content of limestone determined from thermal analysis.

Chemical Composition	Phase Wt. %
SiO_2	15.23
Al_2O_3	3.33
Fe_2O_3	2.75
CaO	64.40
SO_3	1.41
MgO	0.64
K_2O	0.83
CO_2	11.41

Table 4: Mineralogy of Portland-limestone cement used.

Mineralogical Composition	Phase Wt. %
C_3S	60.11
C_2S	7.66
C_3A	9.42
C_4AF	1.03
C\$$H_2$	3.51
$CaCO_3$	18.27

Table 5: Distinguishing properties of the calcium carbonates used.

Calcium Carbonate	Grain Size [μm]	D_{50} [μm]	Crystal System
Micro-calcite	1.5-11.5	7.45	Hexagonal
Nano-calcite	0.090-1.20	0.450	Hexagonal
Amorphous-$CaCO_3$	0.065-0.720	0.205	Non-crystalline

Table 6: Database entries used to produce the capture process inventories for each scenario.

Input	Scenario	Ecoinvent Database Entry*	Quantity
Sodium Hydroxide	1	*Sodium hydroxide, without water, in 50% solution state (RER) chlor-alkali electrolysis, diaphragm cell Alloc Def, U*	0.7991 kg
	2	*Sodium hydroxide, without water, in 50% solution state (RER) chlor-alkali electrolysis, membrane cell Alloc Def, U*	0.7991 kg
Ammonia	3	Ammonia, liquid (RoW) ammonia production, steam reforming, liquid Alloc Def, U	0.104 kg
Calcium Chloride	1,2,3	*Calcium chloride (RER) epichlorohydrin production from allyl chloride Alloc Def, U*	1.0998 kg
Water	1,2,3	*Drinking water, water purification treatment, production mix, at plant from groundwater RER S*	5.0 kg
CO_2	1,2,3	Calculated value	0.4397 kg
Elecricity	1,2	*Electricity, low voltage (GB) market for Alloc Rec, S*	0.087 kWh
	3	*Electricity, low voltage (GB) market for Alloc Rec, S*	0.312 kWh
		*Entries in italics are the names of the Ecoinvent Databse entries as they appear in SimPro	

Table 7: Blaine fineness of OPC, PLC and calcium carbonate blended cements.

	OPC	PLC	Micro-calcite			Nano-calcite			Amorphous-$CaCO_3$		
			5%	10%	15%	5%	10%	15%	5%	10%	15%
Surface area (m^2/kg)	390	410	406	421	439	424	453	487	431	466	492

Table 8: Standard consistency, and setting times of OPC, PLC and calcium carbonate cement blends.

Cement Blend		Standard Consistency (± 0.005)	Initial Set (min ± 1)	Final Set (min ± 5)
OPC		0.265	48	365
PLC		0.250	52	380
	5%	0.270	45	350
Micro-calcite	10%	0.275	43	345
	15%	0.275	41	340
	5%	0.285	42	340
Nano-calcite	10%	0.285	39	320
	15%	0.290	37	305
	5%	0.290	41	335
Amorphous-$CaCO_3$	10%	0.295	39	305
	15%	0.295	35	285

Table 9: Impact assessment categories and their definitions. Definitions from Čuček et al. (2015)

Impact category	Definition
Climate change	Heat absorbed by green house gases measured in kg CO_2 equivalent
Ozone depletion	Measure of potential impact on the ozone layer measured in kg trichlorofluoromethane (CFC-11) equivalent
Human toxicity, non-cancer effects	Potential harm to humans per unit of product excluding carcinogens, measured in Comparative Toxic Unit for humans (CTUh)
Human toxicity, cancer effects	Potential harm to humans from carcinogens produced per unit of product, measured in CTUh
Particulate matter	Mass per cubic metre of air of particles with a diameter less than 2.5 micrometres.
Photochemical ozone formation	Formation of ground-level smog within the troposphere measured in non-methane volatile organic compound (NMVOC) equivalent
Acidification	Sum of NH3, NOx, and SOx emissions throughout the life cycle measured in moles of H^+ equivalent
Terrestrial eutrophication	Sum of nitrogen emissions and flows to land measured in moles of nitrogen equivalent
Freshwater eutrophication	Sum of emissions and flows to freshwater measured in kg of phosphorous equivalent
Marine eutrophication	Sum of nitrogen emissions and flows measured in kg of nitrogen equivalent
Freshwater ecotoxicity	Potential harm to fresh-water ecosystems measured in Comparative Toxic Units ecotoxicity (CTUe)
Land use	Changes in soil organic matter associated with land utilisation measured in kg of carbon in deficit
Water resource depletion	Cubic metres of water required to produce one unit of product
Mineral, fossil & ren resource depletion	Depletion of non-living resources measured in kilograms of antimony equivalent

Table 10: Impact assessment for the production of 1 kg of Portland cement. (Ecoinvent Database entry: *Portland cement (CEM I), CEMBUREAU technology mix, CEMBUREAU production mix, at plant, EN 197-1 RER S*)

Impact category	Unit	Total
Climate change	kg CO_2 eq	0.899172
Ozone depletion	kg CFC-11 eq	$4.4*10^{-8}$
Human toxicity, non-cancer effects	CTUh	$2.55*10^{-8}$
Human toxicity, cancer effects	CTUh	$4.03*10^{-10}$
Particulate matter	kg PM2.5 eq	0.000113
Photochemical ozone formation	kg NMVOC eq	0.00221
Acidification	molc H^+ eq	0.002814
Terrestrial eutrophication	molc N eq	0.008146
Freshwater eutrophication	kg P eq	$2.27*10^{-7}$
Marine eutrophication	kg N eq	0.000701
Freshwater ecotoxicity	CTUe	0.015867
Land use	kg C deficit	0
Water resource depletion	m^3 water eq	$6.32*10^{-5}$
Mineral, fossil & ren resource depletion	kg Sb eq	9.9E-07

Table 11: Impact assessment of carbon capture process for the production of 1 kg $CaCO_3$ using diaphragm cell electrolysis method of NaOH production (scenario 1).

Impact category	Unit	Total
Climate change	kg CO_2 eq	0.667361
Ozone depletion	kg CFC-11 eq	$7.2*10^{-7}$
Human toxicity, non-cancer effects	CTUh	$1.49*10^{-7}$
Human toxicity, cancer effects	CTUh	$1.31*10^{-8}$
Particulate matter	kg PM2.5 eq	0.000585
Photochemical ozone formation	kg NMVOC eq	0.002625
Acidification	molc H^+ eq	0.006484
Terrestrial eutrophication	molc N eq	0.009432
Freshwater eutrophication	kg P eq	0.000118
Marine eutrophication	kg N eq	0.000874
Freshwater ecotoxicity	CTUe	0.45217
Land use	kg C deficit	1.31309
Water resource depletion	m^3 water eq	0.011099
Mineral, fossil & ren resource depletion	kg Sb eq	$6.66*10^{-5}$

Table 12: Impact assessment of carbon capture process for the production of 1 kg $CaCO_3$ using membrane cell electrolysis method of NaOH production (scenario 2).

Impact category	Unit	Total
Climate change	kg CO_2 eq	0.154308
Ozone depletion	kg CFC-11 eq	$6.66*10^{-7}$
Human toxicity, non-cancer effects	CTUh	$1.21*10^{-7}$
Human toxicity, cancer effects	CTUh	$1.07*10^{-8}$
Particulate matter	kg PM2.5 eq	0.000404
Photochemical ozone formation	kg NMVOC eq	0.001574
Acidification	molc H^+ eq	0.003512
Terrestrial eutrophication	molc N eq	0.005737
Freshwater eutrophication	kg P eq	$6.73*10^{-5}$
Marine eutrophication	kg N eq	0.000541
Freshwater ecotoxicity	CTUe	0.368367
Land use	kg C deficit	-0.99831
Water resource depletion	m^3 water eq	0.001789
Mineral, fossil & ren resource depletion	kg Sb eq	$6.16*10^{-5}$

Table 13: Impact assessment for the production of 1 kg of $CaCO_3$ using ammonia as the capture medium (scenario 3).

Impact category	Unit	Total
Climate change	kg CO_2 eq	0.250
Ozone depletion	kg CFC-11 eq	$1.43*10^{-7}$
Human toxicity, non-cancer effects	CTUh	$1.86*10^{-7}$
Human toxicity, cancer effects	CTUh	$2.74*10^{-8}$
Particulate matter	kg PM2.5 eq	0.000374
Photochemical ozone formation	kg NMVOC eq	0.0014
Acidification	molc H^+ eq	0.00354
Terrestrial eutrophication	molc N eq	0.00456
Freshwater eutrophication	kg P eq	0.000209
Marine eutrophication	kg N eq	0.000467
Freshwater ecotoxicity	CTUe	6.5
Land use	kg C deficit	0.855
Water resource depletion	m^3 water eq	0.00251
Mineral, fossil & ren resource depletion	kg Sb eq	$2.26*10^{-5}$

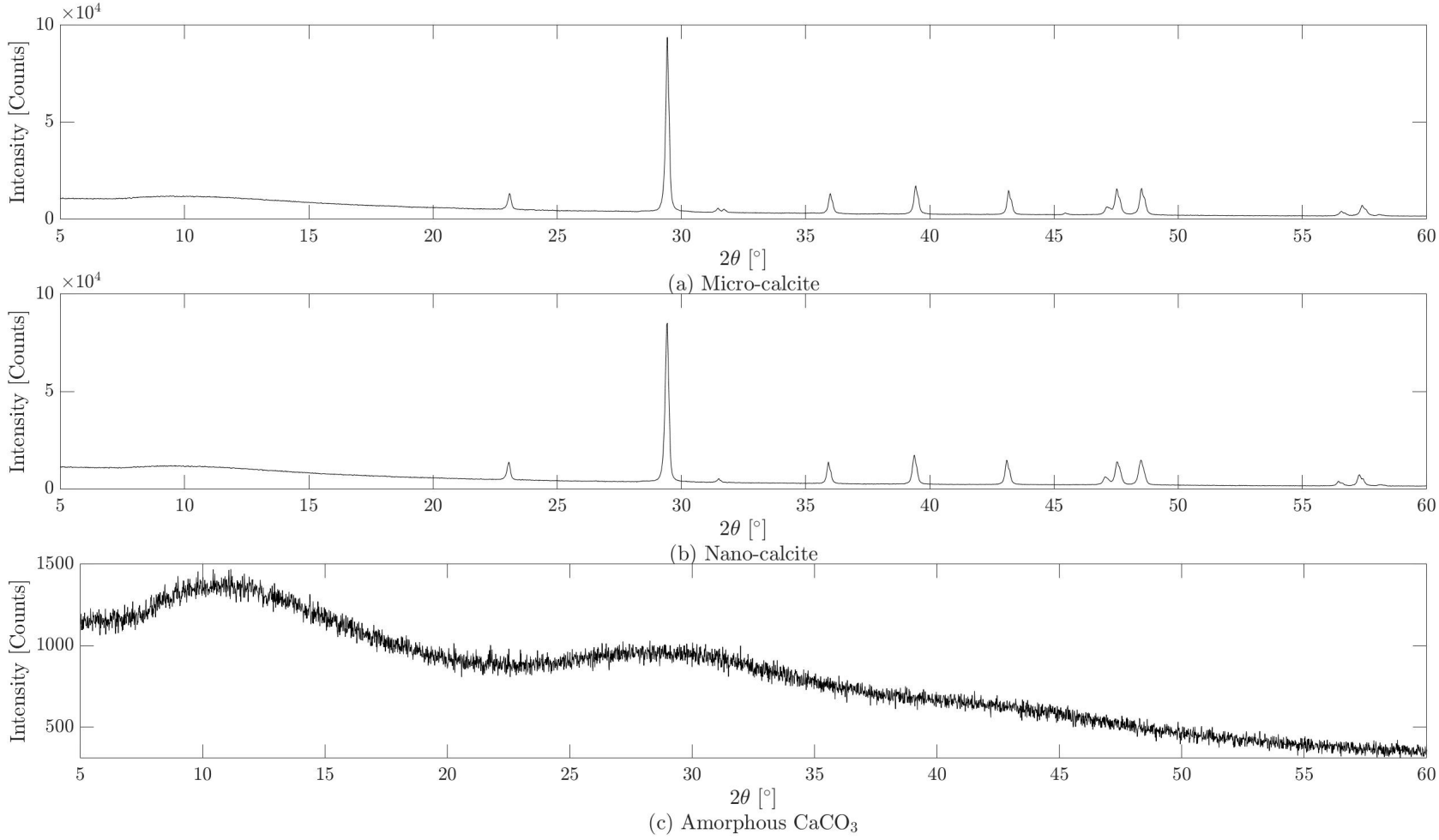

Figure 1: X-ray diffractograms of (a) micro-calcite, (b) nano-calcite and (c) amorphous $CaCO_3$.

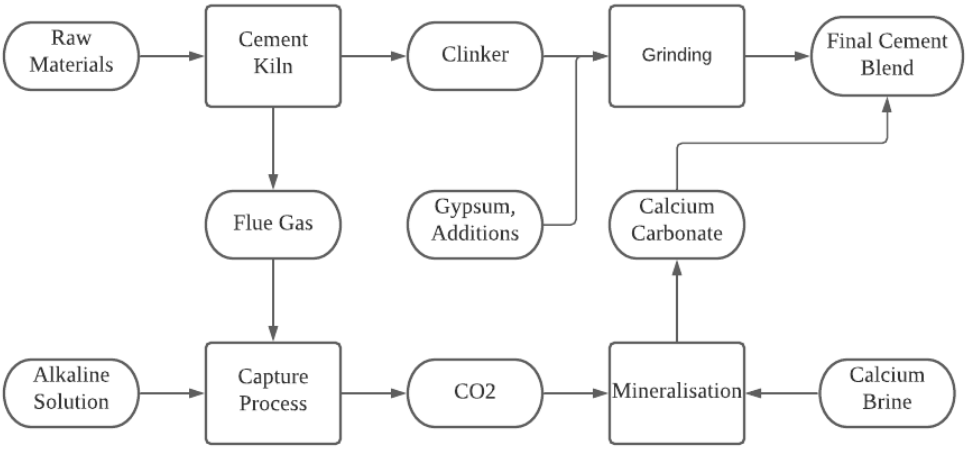

Figure 2: System examined in the scope of this LCA.

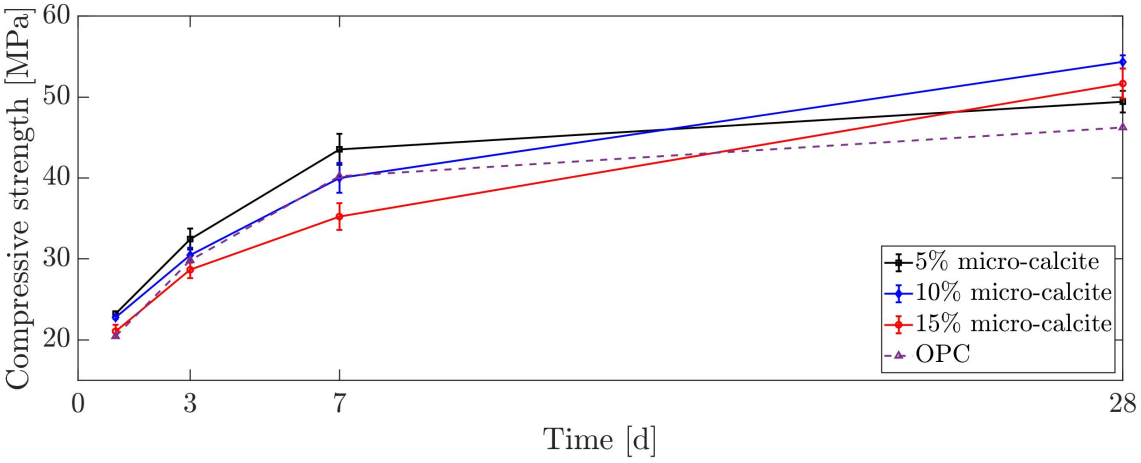

Figure 3: Compressive strength of micro-calcite blends after 3, 7 & 28 days with OPC for reference.

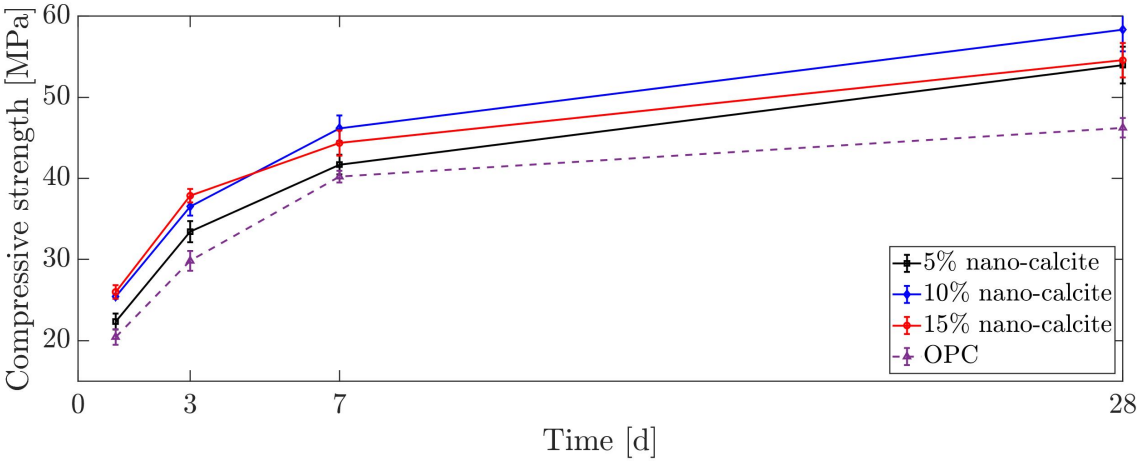

Figure 4: Compressive strength of nano-calcite blends after 3, 7 & 28 days with OPC for reference.

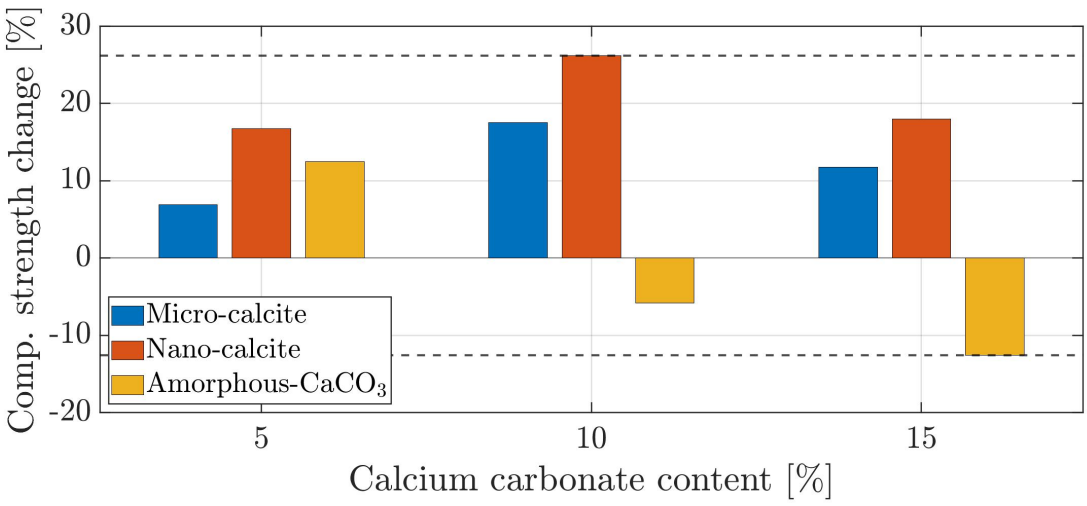

Figure 5: Percentage change of compressive strength of calcium carbonate blends compared to OPC

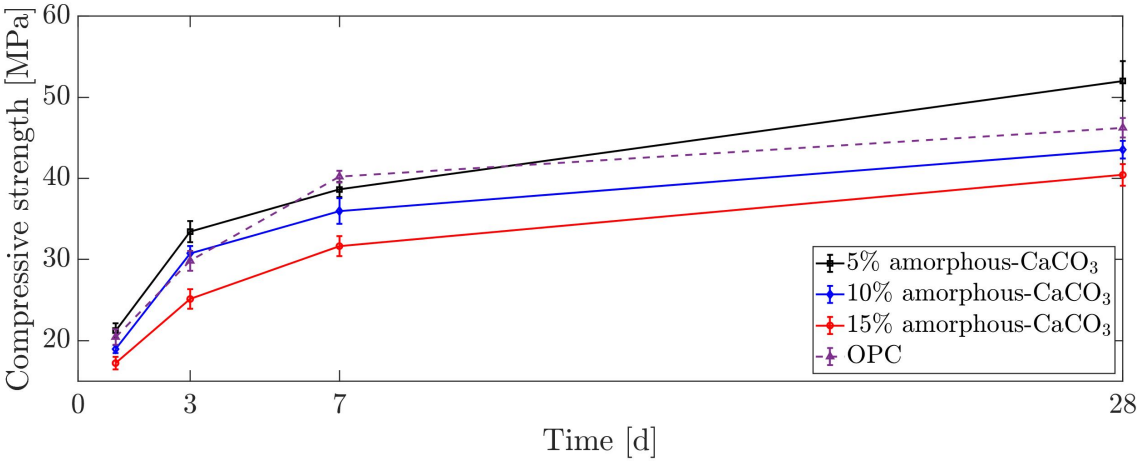

Figure 6: Compressive strength of amorphous-$CaCO_3$ blends after 3, 7 & 28 days with OPC for reference.

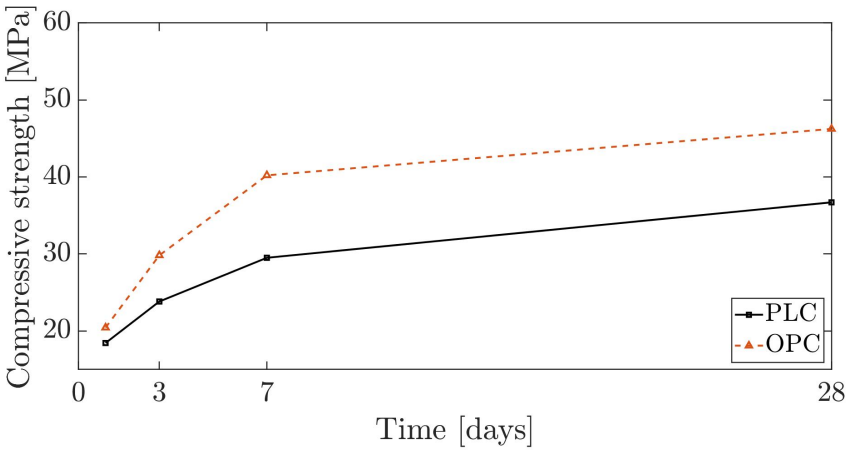

Figure 7: Compressive strength of PLC after 1, 3, 7 & 28 days with OPC for reference.

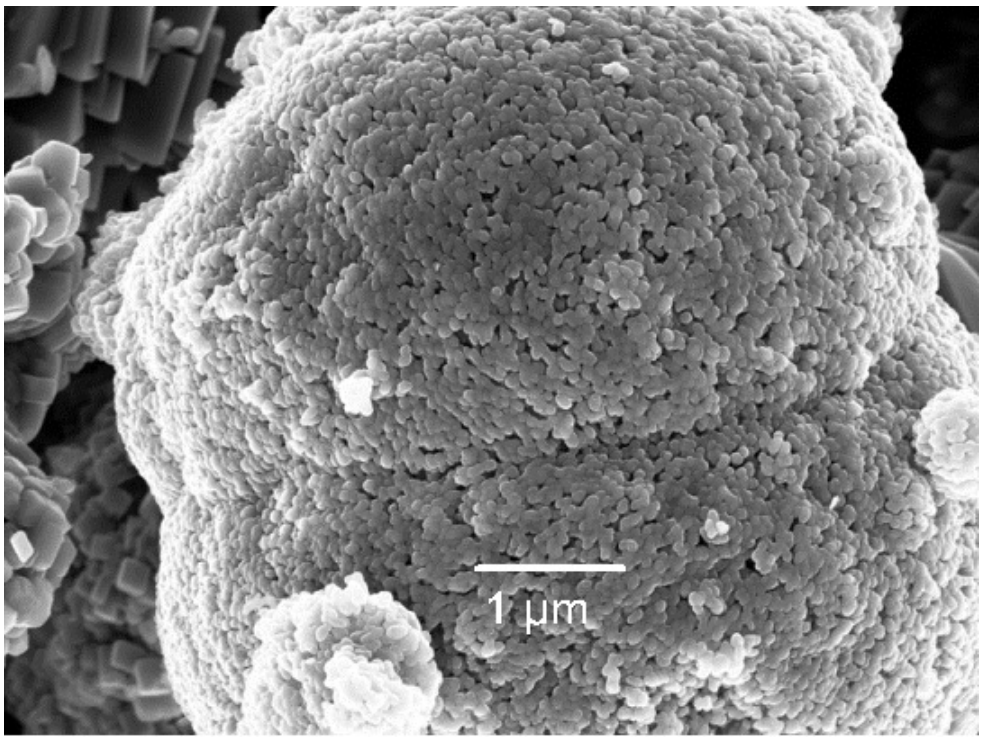

Figure 8: SEM image of amorphous-$CaCO_3$. Agglomeration of smaller particles forming a particle several microns in size. Due to the age of the sample, crystallised $CaCO_3$ is visible in the background.

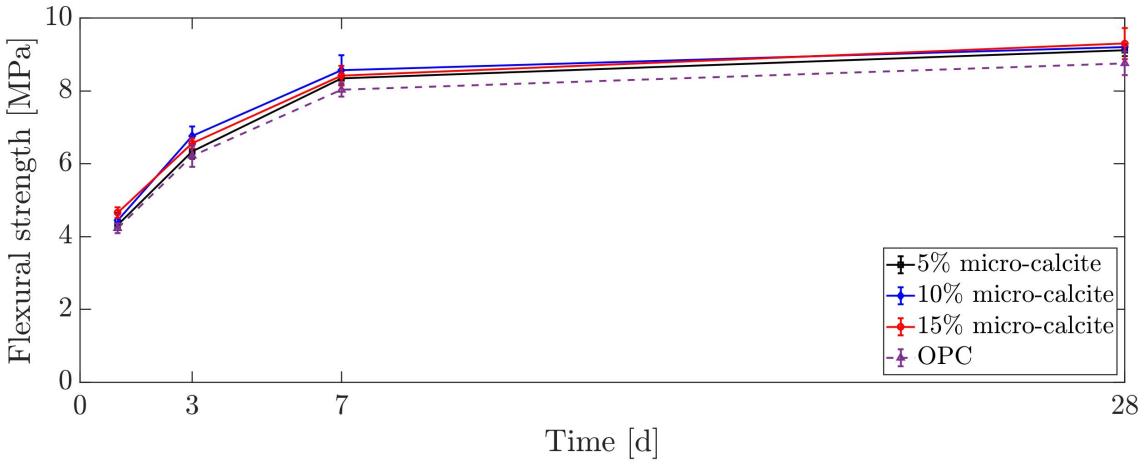

Figure 9: Flexural strength of micro-calcite blends after 1, 3, 7 & 28 days with OPC for reference.

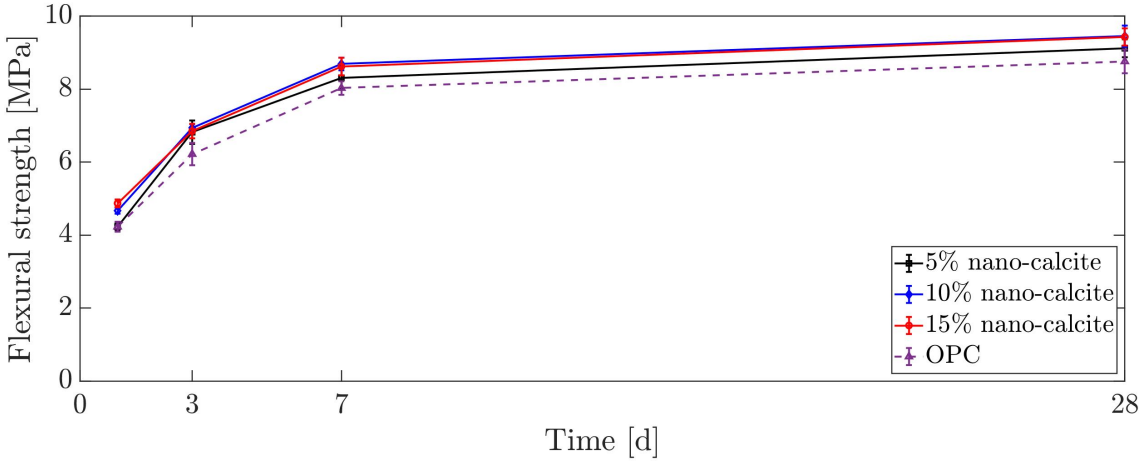

Figure 10: Flexural strength of nano-calcite blends after 1, 3, 7 & 28 days with OPC for reference.

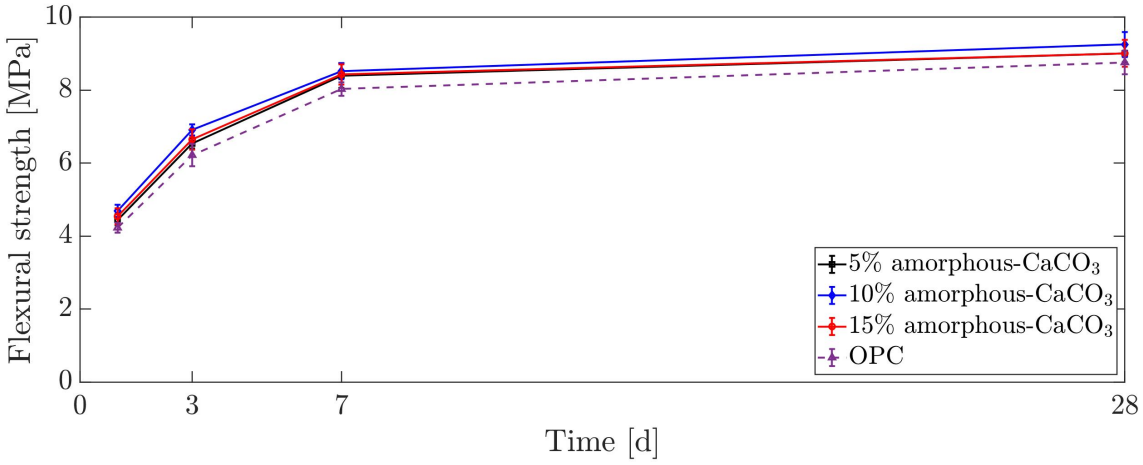

Figure 11: Flexural strength of amorphous-$CaCO_3$ blends after 1, 3, 7 & 28 days with OPC for reference.

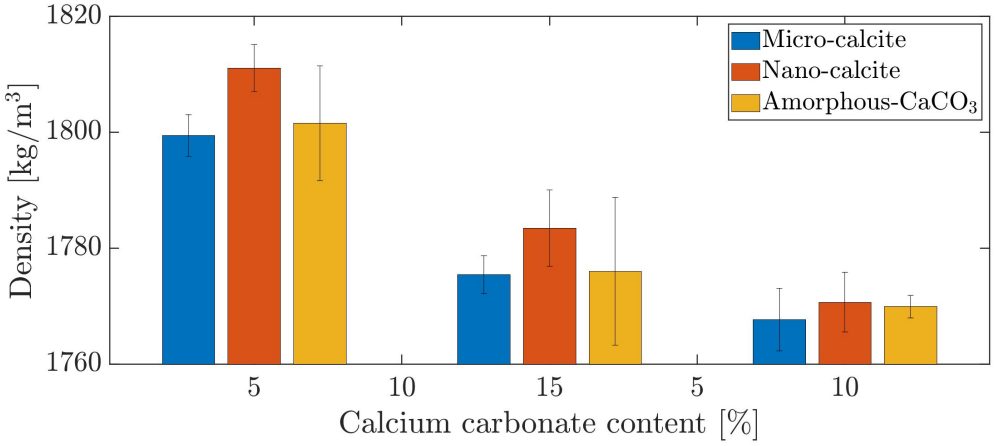

Figure 12: Bulk density of blended cements after curing for 28 days.

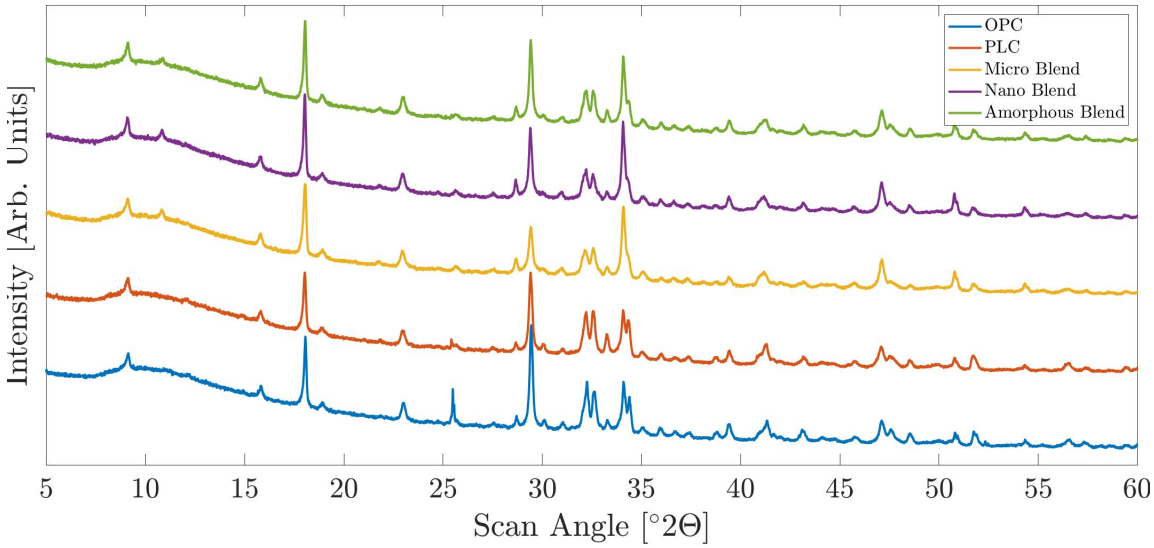

Figure 13: XRD diffractograms of OPC, PLC, and calcium carbonate blends after 7 days of hydration.

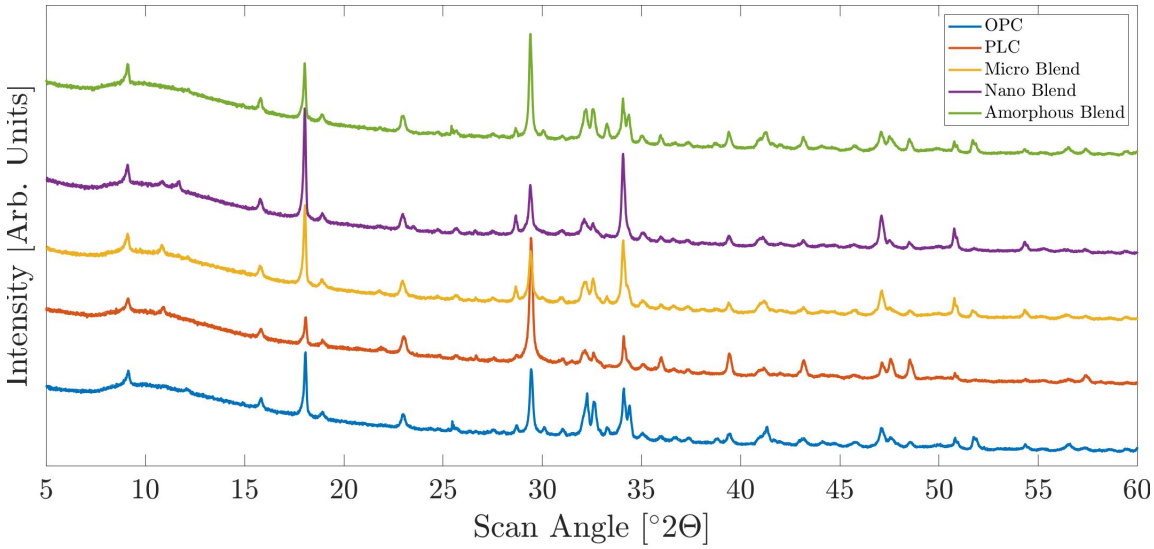

Figure 14: XRD diffractograms of OPC, PLC, and calcium carbonate blends after 28 days of hydration.

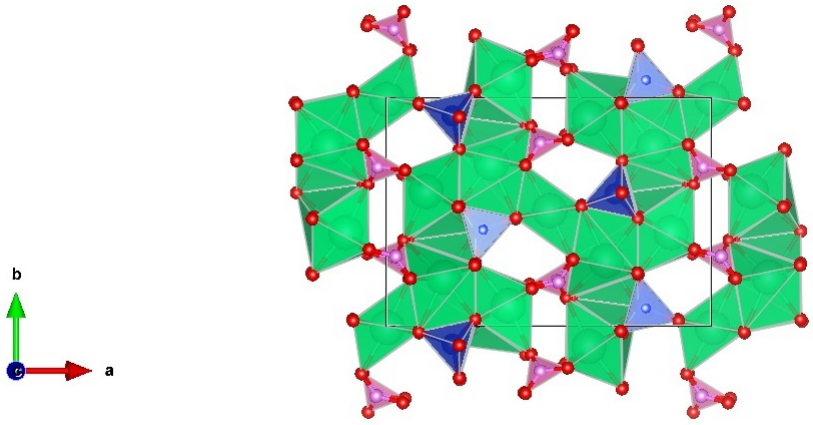

Figure 15: Generated structure of tilleyite viewed along the c plane from the atom positions obtained from Rietveld refinement of nano-calcite blended cement shown in figure 14.

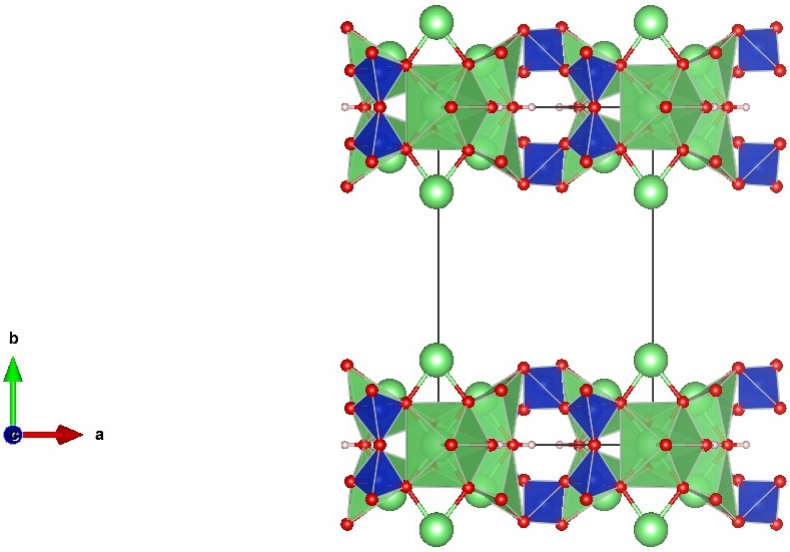

Figure 16: Generated structure of scawtite viewed along the c plane from the atom positions obtained from Rietveld refinement of nano-calcite blended cement shown in figure 14.

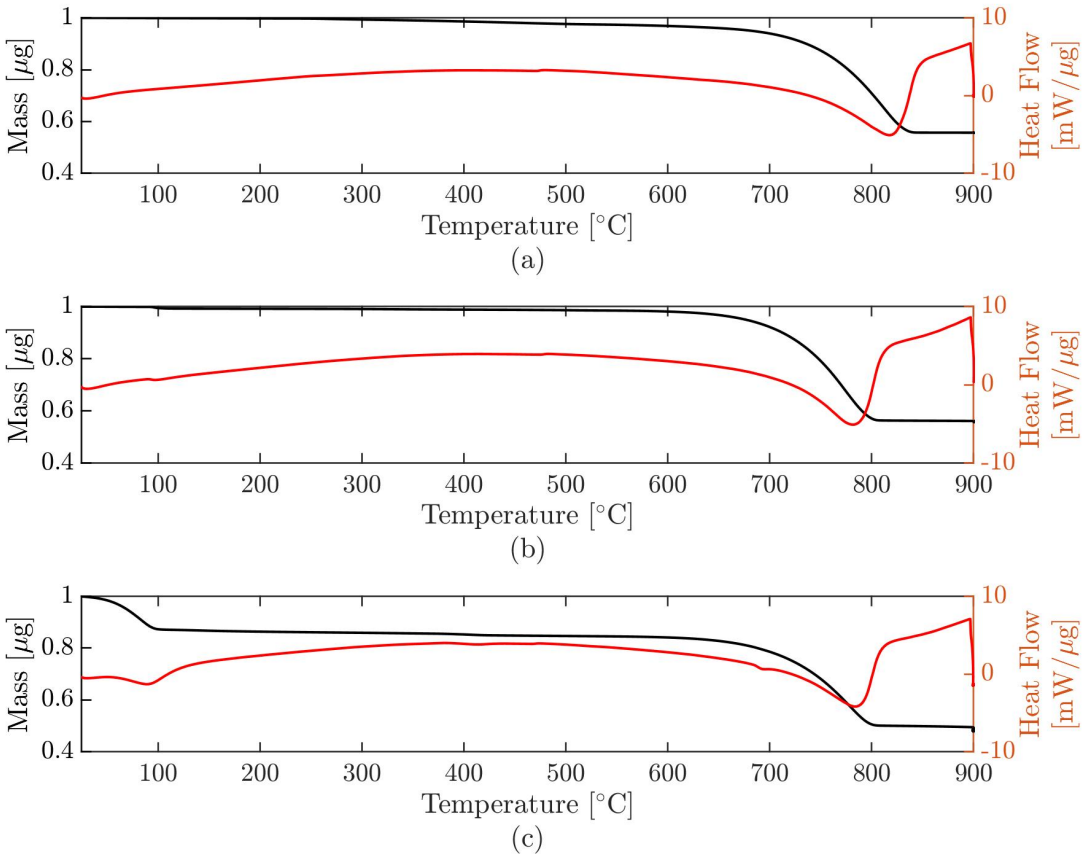

Figure 17: Thermal analysis of calcium carbonates prior to blending with OPC. (a) micro-calcite, (b) nano-calcite and (c) amorphous-$CaCO_3$.

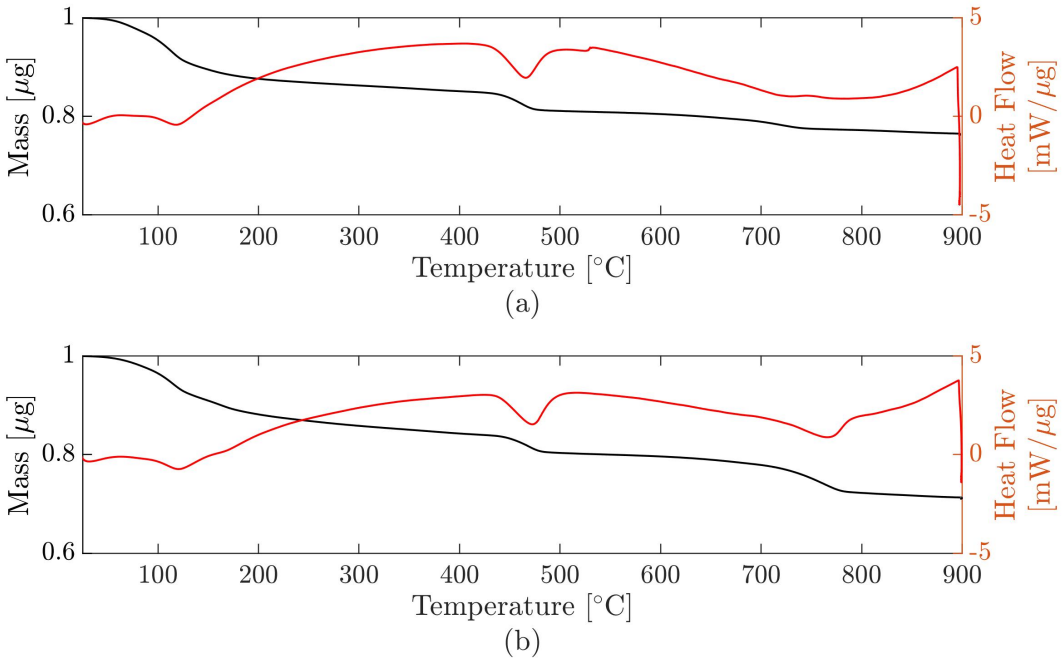

Figure 18: Thermals analysis of OPC and PLC cured for 7 days. (a) OPC and (b) PLC.

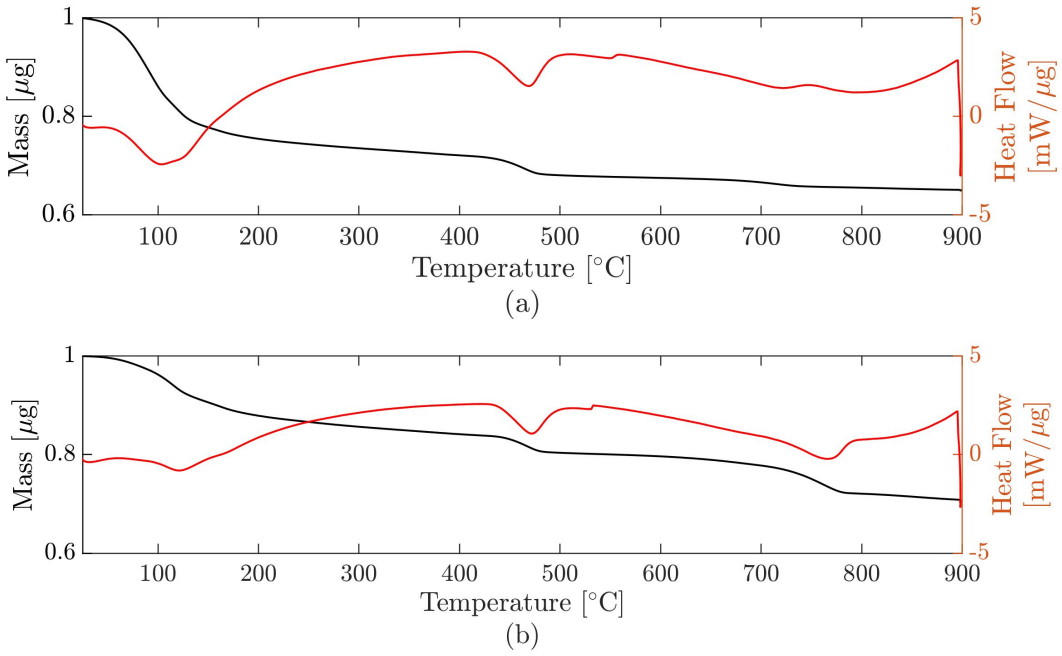

Figure 19: Thermals analysis of OPC and PLC cured for 28 days. (a) OPC and (b) PLC.

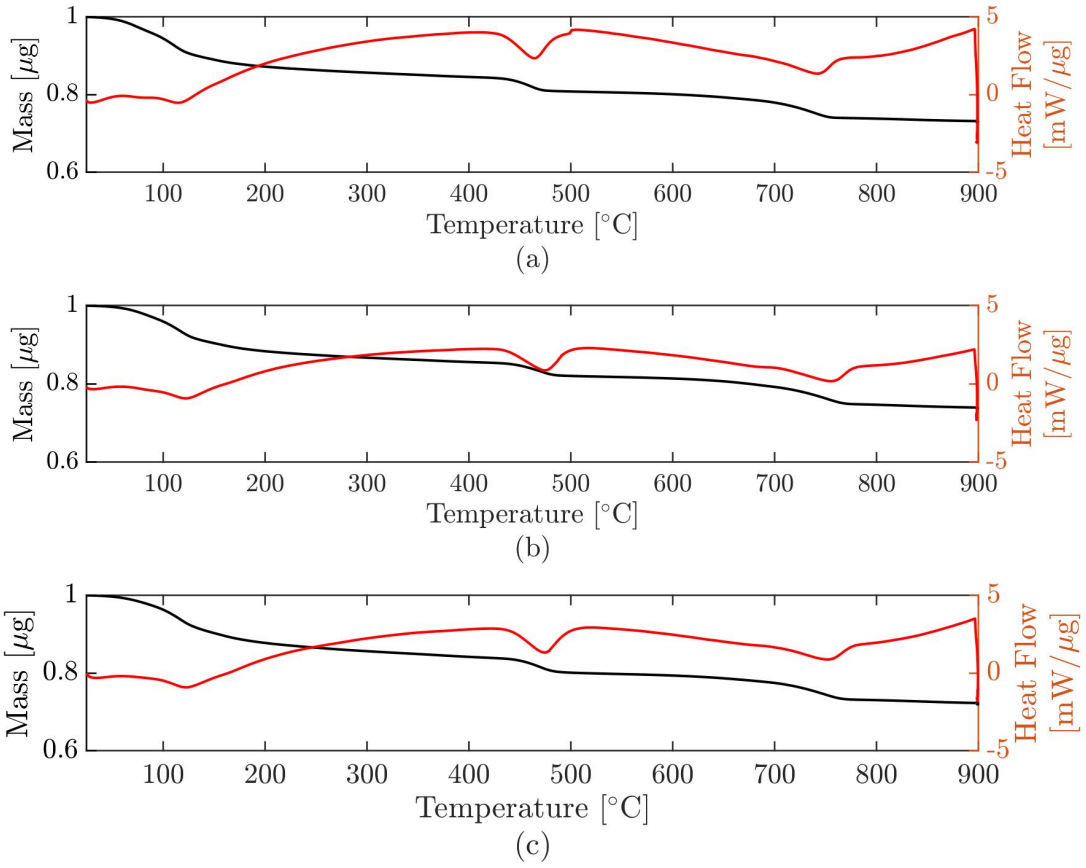

Figure 20: Thermal analysis of calcium carbonate Portland cement blends after 7 days of curing. (a) micro-calcite Portland cement, (b) nano-calcite Portland cement and (c) amorphous-$CaCO_3$.

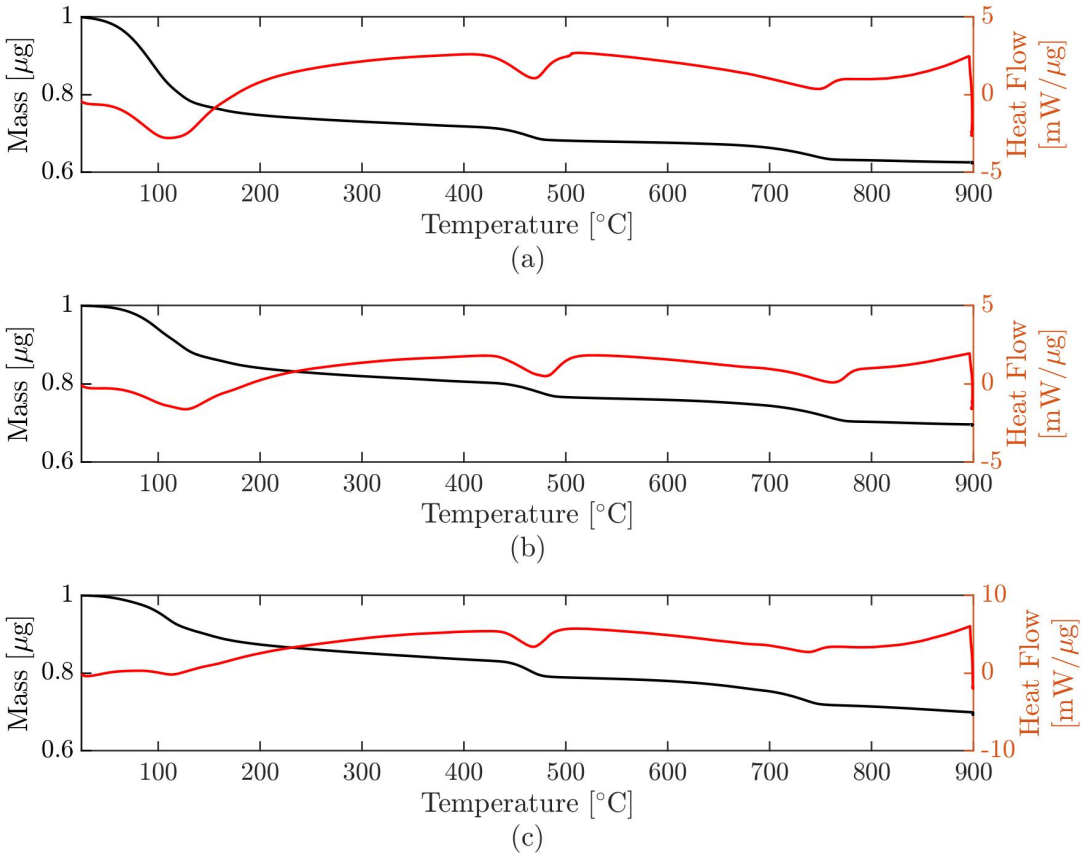

Figure 21: Thermal analysis of calcium carbonate Portland cement blends after 28 days of curing. (a) micro-calcite Portland cement, (b) nano-calcite Portland cement and (c) amorphous-$CaCO_3$.